*J. Fluid Mech.* (1992), *vol.* 243, *pp.* 443–455
*Printed in Great Britain*



# Stability of Taylor–Dean flow in a small gap between rotating cylinders

By FALIN CHEN AND M. H. CHANG
Institute of Applied Mechanics, National Taiwan University, Taipei, Taiwan 10764, ROC

(Received 31 July 1991 and in revised form 25 March 1992)

A linear stability analysis has been implemented for Taylor–Dean flow, a viscous flow between rotating concentric cylinders with a pressure gradient acting in the azimuthal direction. The analysis is made under the assumption that the gap spacing between the cylinders is small compared to the mean radius (small-gap approximation). A parametric study covering wide ranges of $\mu$, the ratio of angular velocity of the outer cylinder to that of inner cylinder, and $\beta$, a parameter characterizing the ratio of representative pumping and rotation velocities is conducted. For $-1 \leqslant \mu < 1$, results show that non-axisymmetric instability modes prevail in a wide range of $\beta$. The most stable state is found to occur within $-3.9 < \beta < -3.6$ for $\mu < 0.3$ and at $-\beta \approx 1.59\mu + 3.5$ for $\mu > 0.3$. The most stable state is always accompanied by a shortest critical axial wavelength. Instability modes with different azimuthal wavenumber have similar stability characteristics because the basic state is either close to or at the most stable situation. This similarity is absent from either Taylor or Dean flow.

## 1. Introduction

The stability of a viscous flow between two concentric cylinders is of both academic and engineering application interest. Couette (1890) initiated the investigation of the flow in an annulus between two rotating cylinders for bearing lubrication and viscometry. Taylor (1923) considered the stability problem both experimentally and theoretically and obtained a criterion for the onset of a secondary motion in the form of cellular toroidal vortices spaced regularly along the axis of the cylinder (Taylor problem). Another similar type of secondary flow may occur between two concentric cylinders when a viscous flow is driven by an azimuthal pressure gradient (Dean problem). This problem was first studied by Dean (1928) and had been considered again by Hammerlin (1958) and Reid (1958). Walowit, Tsao & DiPrima (1964) studied both the Taylor and Dean problems for arbitrary gap spacings. The Taylor–Dean problem is concerned with the stability of a viscous flow between two concentric cylinders, in which the basic flow (referred as Taylor–Dean flow) is the combination of a circular Couette flow and an azimuthal Poiseuille flow. A detailed measurement of an azimuthal velocity profile of the basic flow is available in Chen *et al.* (1990). As far as engineering application is concerned, the flow driven by both rotating cylinder(s) and an azimuthal pressure gradient can be found in, for example, an electrogalvanizing line in the steel-making industry which uses a roller-type cell to plate zinc onto the surface of a steel strip (Komoda 1983; Nabatame 1984) and in a rotating drum filter in the paper- and board-making industry in which a sheet of fibre off a drum rotating in a vat full of fibre suspensions (Brewster & Nissan 1958). Paper-making engineering used to observe that longitudinal streaks regularly

spaced along the axis of the drum arise in the sheet formed, which are obviously resulted from the secondary fluid motion predominating in the curved passage.

The Taylor–Dean problem was first studied experimentally by Brewster & Nissan (1958) and both experimentally and theoretically by Brewster, Grosberg & Nissan (1959). The small-gap approximation was assumed in their theoretical analyses. Later, the theoretical analysis was extended by DiPrima (1959), using the Fourier expansion technique to study the problem with the small-gap approximation in a larger range of $\beta$ (to be defined in §2) and by Meister (1962) as well as Sparrow & Lin (1965) using a shooting technique to attack the problem for arbitrary gap spacings. All these studies considered the onset of instability to be axisymmetric as well as stationary and were restricted to the case of $\mu = 0$, in which the inner cylinder is rotating while outer cylinder is fixed.

Of particular interest is the result obtained by DiPrima (1959) that the flow is most stable near $\beta = -3.5$, at which the critical wavenumber ($a^c$) jumps discontinuously from 5.8 to 7.4 as $\beta$ decreases. Chandrasekhar (1961) proposed a physical explanation for the sharp maximum of $T^c$ occurring at $\beta = -3.5$ by examining the extent of instability zones in the annulus. On the other hand, to explain the rather peculiar dependence of $a^c$ on $\beta$, Kurzweg (1963), on the basis of Rayleigh's criterion (Rayleigh 1916), noted analytically that the larger $a^c$ corresponds to the instability occurring in the region near inner cylinder and the smaller $a^c$ is related to the instability in the region near outer cylinder. Hughes & Reid (1964) found that the discontinuity of $a^c$ arises because the neutral curve consists of two separated branches (see the circle-solid curves in figure 1) and the maximum of $T^c$ as well as the jump of $a^c$ occurs precisely at $\beta^* = 3.667$. The peculiar topology of the separated neutral curves near $\beta^*$ was re-examined by Raney & Chang (1971) by considering the possible existence of the oscillatory instability modes. They showed that oscillatory axisymmetric modes exist of stability approximately equal to that of a steady mode very close to $\beta^*$ (see the triangle-dash curve in figure 1). They also indicated that, although the resulting reduction of the value of $T^c$ is not significant, the most critical mode is oscillatory non-axisymmetric with $m = 1$ in $-3.850 < \beta < -3.635$. Recently, Kachoyan (1987) has implemented an extensive study on the neutral curve topology and pointed out that the separated neutral curves are connected at $\beta \geqslant -3$.

In fact, a fully developed Taylor–Dean flow in an annulus seems to be artificial because, under any circumstance, to provide an external pressure gradient in the azimuthal direction there must be an associated breakdown of the symmetry of the geometry of annulus, which makes a fully developed basic flow impossible. However, the Taylor–Dean flow may in reality exist in a portion of the annulus, such as the flow in eccentric rotating cylinders (see figure 16 of Vohr 1968) or the flow in a partially filled horizontal annulus (Chen *et al.* 1990). Mutabazi *et al.* (1989) implemented a linear stability analysis for the Taylor–Dean flow in the latter configuration, in which the averaged velocity due to the rotating cylinders is equal to, but opposite in direction to, the averaged velocity due to the pressure gradient caused by the free surface within the gap; namely, $\beta = -3$. They considered the instability to arise from oscillatory and axisymmetric modes. To study the flow pattern formation as well as the transition from the basic state to disorder, Mutabazi *et al.* (1988, 1990, 1991) conducted a series of experiments for a variety of $\mu$ in the same configuration. They indicated that some sort of nonlinear interaction such as spatiotemporal pattern modulation may exist in Taylor–Dean flow.

In the present study, we consider a fully developed Taylor–Dean flow within a small-gap coaxial annulus. A complete linear stability analysis with the small-gap

approximation is implemented, in which three-dimensional disturbances of both stationary and oscillatory modes are considered. We first compare the calculated results with those of previous studies and show that the most unstable mode for $\mu = 0$ near $\beta^*$ is non-axisymmetric with $m = 5$ (see the square-dash curve in figure 1). A systematic parameter study which covers $-1 \leqslant \mu \leqslant 1$ and $-10 \leqslant \beta \leqslant 10$ is then carried out. Results provide an overview of the general stability characteristics and the nature of the non-axisymmetric modes as well as the corresponding travelling waves in the azimuthal direction.

## 2. Problem formulation and method of solution

We consider two infinitely long concentric circular cylinders with the $z$-axis as their common axis and let $R_1$ and $R_2$ denote the radii of the inner and outer cylinders, respectively. The flow in the annulus is driven simultaneously by rotating the inner and outer cylinders and by an azimuthal pressure gradient. A cylindrical coordinate system is chosen which is usually denoted by $r$, $\theta$, and $z$. If $U_r$, $U_\theta$, and $U_z$ are the velocity components in the increasing $r$-, $\theta$-, and $z$-directions, the Navier–Stokes equations admit a steady solution in terms of the velocities of the three components:

$$U_r = U_z = 0, \quad U_\theta = V(r). \tag{1}$$

The basic state velocity $V(r)$, a combination of the fully developed velocity distributions of circular Couette and azimuthal Poiseuille flows, is given by

$$V(r) = Ar + \frac{B}{r} + \frac{1}{2\rho\nu}\frac{\partial P}{\partial \theta}\left(r\ln r + Cr + \frac{E}{r}\right), \tag{2}$$

where $\rho$, $\nu$, and $P$ are the density and kinematic viscosity of the fluid, and the pressure of the basic flow, respectively. The constants are

$$A = \Omega_1 \frac{\mu - \eta^2}{1-\eta^2}, \quad B = \Omega_1 R_2^2 \eta^2 \frac{1-\mu}{1-\eta^2}, \quad C = -\frac{\ln R_2 - \eta^2 \ln R_1}{1-\eta^2}, \quad E = -\frac{R_1^2}{1-\eta^2}\ln\eta. \tag{3}$$

The $\partial P/\partial\theta$ in (2) accounts for the basic-state azimuthal pressure gradient due to external pumping and $\eta$ is the ratio of radii, $R_1/R_2$. Note that the pressure may not be single-valued, i.e. $P(\theta + 2\pi) \neq P(\theta)$, if free surfaces exist within the gap (Mutabazi *et al.* 1989). In the present study, we assume that the gap between the two cylinders $d = R_2 - R_1$, is much smaller than the mean radius $R_0 = \frac{1}{2}(R_1 + R_2)$. Consequently, after taking the limit $\eta \to 1$ and some further manipulation, we obtain

$$V(r) = r\Omega_1[1 - (1-\mu) + \beta x(1-x)], \tag{4}$$

where $x = (r - R_1)/d$ and $\beta = 3(1+\mu)\, V_P/V_R$, in which $V_R = \frac{1}{2}R_1\Omega_1(1+\mu)$ and $V_P = -(\partial P/\partial\theta)(d^2/12\nu R_1)$ are the average velocities due to rotation and pumping, respectively.

To study the stability of this flow we superimpose a general disturbance on the basic solution, substitute in the equations of motion and the continuity equation and neglect quadratic terms. Since the coefficients in the resultant disturbance equations depend only on $r$, it is possible to look for solutions of the form

$$u_\theta = V(r) + v(r)\exp[\mathrm{i}(st + m\theta + \lambda z)], \tag{5}$$

where $v(r)$ is the azimuthal component of the small disturbance velocity, and with similar expressions for the other components of velocity and the pressure. Note that

$m$ may be a non-integer as the partially filled gap configuration is considered (Mutabazi *et al.* 1989). However, for the present case of fully developed Taylor–Dean flow, we can take $m$ to be zero or a positive integer. The parameter $s$ is in general complex and $\lambda$ is real.

We now introduce the dimensionless variables

$$\delta = \frac{d}{R_1}, \quad a = \lambda d, \quad \sigma = \frac{sd^2}{\nu}, \quad k = \left(-\frac{\Omega_1}{4A}\right)^{\frac{1}{2}} m, \quad T = -\frac{4A\Omega_1 d^4}{\nu^2}. \tag{6}$$

Since the small-gap approximation yields $A = -\Omega_1(1-\mu)/2\delta$ plus terms $O(1)$, we have asymptotically

$$k \sim [\delta/2(1-\mu)]^{\frac{1}{2}} m, \quad T \sim 2(1-\mu)\,(\Omega_1 R_1 d/\nu)^2 \delta, \tag{7}$$

which account for the scaling of the azimuthal wavenumber and the Taylor number, respectively. After eliminating the perturbations in the pressure and the axial velocity, and letting $(\nu/2\Omega_1 a^2 d^2)u$ be replaced by $u$, the radial component of small disturbance velocity, we obtain the following sixth-order system of ordinary differential equations (ODEs):

$$\mathrm{L}(\mathrm{D}^2 - a^2)\, u = K(x)\, v, \tag{8}$$

$$\mathrm{L}v = -a^2 T\left[1 - \frac{\beta}{1-\mu}(1-2x)\right] u, \tag{9}$$

where $\mathrm{D} = \mathrm{d}/\mathrm{d}x$ and

$$\mathrm{L} = \mathrm{D}^2 - a^2 - \mathrm{i}[\sigma + kT^{\frac{1}{2}} K(x)] \tag{10}$$

and

$$K(x) = 1 - (1-\mu)\, x + \beta x(1-x). \tag{11}$$

The boundary conditions at $x = 1$ and $x = 0$ are

$$u = \mathrm{D}u = v = 0. \tag{12}$$

Note that as $\beta = 0$, equations (8) and (9) are identical with those of the Taylor problem as described in Krueger, Gross & DiPrima (1966).

The ODEs (8) and (9) with the boundary conditions (12) determine an eigenvalue problem of the form

$$F(\mu, \beta, k, a, \sigma, T) = 0. \tag{13}$$

The marginal state is characterized by $\sigma_{\mathrm{i}}$, the imaginary part of $\sigma$, equal to zero. For given values of $\mu$ and $\beta$, which determine the basic-state velocity, we seek the minimum real positive $T$ over real $a > 0$ and real $k \geqslant 0$, for which there is a solution for (13) with $\sigma_{\mathrm{i}} = 0$. The value of $T$ sought is the critical Taylor number $T^{\mathrm{c}}$ for assigned values of $\beta$ and $\mu$. The values of $a$ and $k$ corresponding to $T^{\mathrm{c}}$ determine the form of the critical disturbance. Since the small-gap approximation is assumed, we have $\delta \to 0$. For a given value of $\delta \ll 1$ ($\delta = 0.05$ is chosen for the present study, see Krueger *et al.* 1966), it has physical meaning only for values of $k$ corresponding to positive integer or zero values of the azimuthal wavenumber $m$. Moreover, the real part of $\sigma$, namely $\sigma_{\mathrm{r}}$, corresponding to $T^{\mathrm{c}}$ determines the frequency of the oscillation as well as the angular velocity of the travelling wave. We work with the dimensionless wave speed $c = -\sigma_{\mathrm{r}}/kT^{\frac{1}{2}} = -s_{\mathrm{r}}/m\Omega_1$, which in essence accounts for the angular velocity of the travelling wave relative to the angular velocity of the rotating inner cylinder. We solve the two-point eigenvalue problem defined by (8)–(12) by a shooting technique together with an unit-disturbance method. This method has been used by, for example, DiPrima (1955), Harris & Reid (1964), Sparrow, Munro &

Jonsson (1964), and Krueger *et al.* (1966) for similar hydrodynamic stability problems. For details the reader is referred to either Harris & Reid or Krueger *et al.*. Note that for obtaining a faster convergence of the iteration, instead of using an algorithm like the bivariate interpolation used by Krueger *et al.* (1966), we use a hybrid algorithm developed by Powell (1970 p. 87) on the basis of a Newton–Raphson scheme as well as the steepest-descent iteration.

## 3. Results and discussion

### 3.1. *Verification of the computer code*

Krueger *et al.* (1966) studied the instability of Taylor flow with respect to non-axisymmetric disturbances, which is a special case of the present Taylor–Dean problem with $\beta = 0$. We thus conduct calculations for $\beta = 0$ and check the results in terms of $T^c$, $a^c$, and $\sigma_r$ with the corresponding data obtained by Krueger *et al.* (table 1). It is shown that for several selected $k$, which are associated with $m = 0$–5, the comparison is in excellent agreement. Another check is made possible by considering the instability with respect to axisymmetric disturbance for small-gap Taylor–Dean problem as done by DiPrima (1959). By assuming $m = 0$, we obtain the characteristic values $T^c$ and $a^c$ for various $\beta$, which again agree very well with those of DiPrima. The only investigation considering non-axisymmetric instability (for $m = 1$ only, unfortunately) for the small-gap Taylor–Dean problem has been done by Raney & Chang (1971). Their results are also confirmed by our calculations.

### 3.2. *Non-axisymmetric oscillatory modes for* $\mu = 0$

For $\mu = 0$ and near $\beta^* = -3.667$, the neutral curve for stationary axisymmetric modes has two branches shown in figure 1 as the circle-solid curves. For $\beta = -3.65$ (figure 1*a*), $T^c$ is determined by the right-hand branch and for $\beta = -3.7$ (figure 1*c*) by the left-hand branch; at $\beta^*$, both branches have approximately equal $T^c$. As a result, at $\beta^*$, the $a^c$ of the axisymmetric mode experiences a dramatic change from 7.8 to 5.7 and $T^c$ reaches a maximum (see the circles shown in figure 2*a*, *b*). Raney & Chang (1971) showed that a neutral curve exists corresponding to oscillatory axisymmetric modes lying between two branches (see the triangle-dash curve shown in figure 1). At $\beta^*$, both stationary and oscillatory axisymmetric modes are of approximately equal stability. In the present study by considering the possible existence of non-axisymmetric modes, we find that the most unstable mode near $\beta^*$ is non-axisymmetric with $m = 5$, which is an instability mode with five waves travelling in the azimuthal direction. As shown in figures 1(*a*–*c*), the value of $T$ of the neutral curve (square-dash) for $m = 5$ is invariably lower than that of either the stationary or oscillatory axisymmetric mode.

By extending the consideration to a larger range, $-10 \leqslant \beta \leqslant 10$, we find that the stability of Taylor–Dean flow is dominated by non-axisymmetric modes in $-4 \leqslant \beta \leqslant -2.2$, in which the azimuthal wavenumber $m$ varies from 1 to 5 depending on $\beta$. We present the $T^c$ and associated $a^c$ for $-10 \leqslant \beta \leqslant 10$ in figures 2(*a*) and 2(*b*), respectively, in which the solid curve represents the critical values corresponding to the axisymmetric mode and the dot curve accounts for those corresponding to non-axisymmetric modes. The circles are the results obtained by DiPrima (1959) for the axisymmetric mode. As one can see, the $T^c$ associated with non-axisymmetric instability is generally smaller than the corresponding one for an axisymmetric disturbance and is closer to the experimental data obtained by Brewster *et al.* (1959), see figure 1 of DiPrima. The stability characteristics in terms of $T^c$ as shown in figure

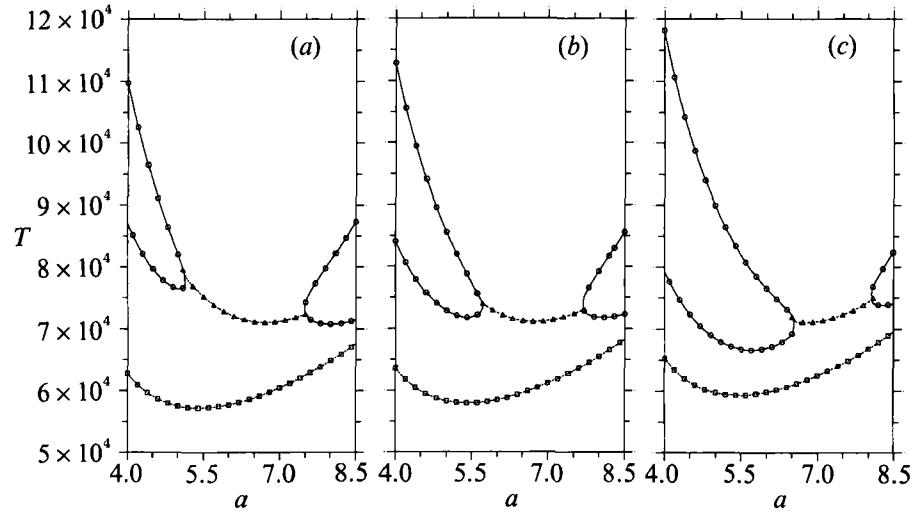


FIGURE 1. Neutral curves for $\mu = 0$ and various $\beta$: —○—, axisymmetric stationary mode $m = 0$ (Hughes & Reid 1964); – – – △– – –, axisymmetric oscillatory mode $m = 0$ (Rayney & Chang 1971); – – –□– – –, non-axisymmetric mode $m = 5$ (present study). (*a*) $\beta = -3.65$; (*b*) $\beta = \beta^* = -3.667$; (*c*) $\beta = -3.7$.

| | | $a^c$ | | $T^c$ | | $-\sigma_r$ | |
|---|---|---|---|---|---|---|---|
| $\mu$ | $k$ | A | B | A | B | A | B |
| 0 | 0 | 3.127 | 3.127 | 3389.9 | 3390.1 | 0 | 0 |
| | 0.15811 | 3.13 | 3.131 | 3402.3 | 3402.5 | 4.8459 | 4.8534 |
| | 0.31623 | 3.14 | 3.143 | 3440.1 | 3440.3 | 9.7675 | 9.7661 |
| | 0.47434 | 3.16 | 3.163 | 3504.7 | 3504.8 | 14.799 | 14.799 |
| | 0.63246 | 3.19 | 3.190 | 3598.5 | 3598.6 | 20.024 | 20.020 |
| | 0.79057 | 3.23 | 3.225 | 3725.5 | 3725.6 | 25.515 | 25.505 |
| −1.0 | 0 | 4.00 | 3.999 | 18663 | 18669 | 0 | 0 |
| | 0.11180 | 3.94 | 3.941 | 18472 | 18478 | 6.3458 | 6.3375 |
| | 0.22361 | 3.80 | 3.799 | 17965 | 17970 | 12.128 | 12.127 |
| | 0.33541 | 3.68 | 3.675 | 17401 | 17404 | 17.028 | 17.013 |
| | 0.44721 | 3.64 | 3.642 | 17126 | 17129 | 21.263 | 21.297 |
| | 0.55901 | 3.69 | 3.686 | 17345 | 17345 | 25.632 | 25.600 |

TABLE 1. Comparison between the results of present study (A) and those of Krueger *et al.* (1966) (B) for Taylor problem $\beta = 0$

2(*a*) illustrate that the stability of Taylor–Dean flow increases monotonically with decreasing $\beta$ for $\beta < -3.743$ but its stability decreases otherwise. The maximum of $T^c$ occurs at $\beta = \beta_{max} = -3.743$, at which the critical axial wavenumber $a^c$ also reaches the maximum. The dot curve of $a^c$ shows several discontinuities in slope, each of which is associated with a switch between two different non-axisymmetric modes. Near $\beta_{max}$, the value of $a^c$ for the non-axisymmetric mode does not have as large a jump as the axisymmetric mode. In general, as with $T^c$, the $a^c$ corresponding to a non-axisymmetric disturbance is smaller than that for an axisymmetric one.

To explain physically the occurrence of the sharp maximum of $T^c$, Chandrasekhar (1961) argued that the value of $\beta$ at which $T^c$ reaches its maximum value should lie near $\beta = -3$ since there, based on Rayleigh's criterion, the layers of stable and

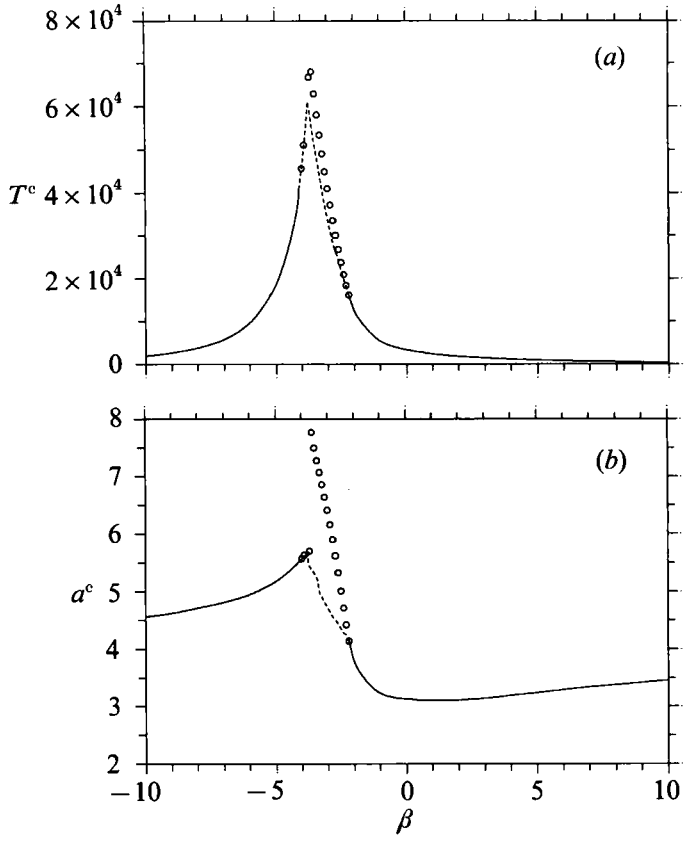


FIGURE 2. Variations of $T^c$ and $a^c$ with $\beta$ for $\mu = 0$: ——, axisymmetric mode; – – –, non-axisymmetric mode; ○, axisymmetric mode by DiPrima (1959). (*a*) $T^c$; (*b*) $a^c$.

unstable fluid are of equal extent within the gap (see Chandrasekhar, figure 94, p. 356). When applied to the case $\mu \neq 0$, however, Hughes & Reid (1964) showed that this argument becomes less compelling. For the present case, which considers viscous effects on the stability characteristics in contrast to the inviscid-flow assumption made for determining Rayleigh's criterion, the maximum of $T^c$ occurs at $\beta = -3.743$. DiPrima (1959) proposed the more promising physical explanation that the most stable state occurs at $\beta_{\max}$ ($-3.667$ according to his computation for axisymmetric mode), because, as long as the average velocities of pumping and rotation are nearly equal but opposite in sign (note that $\beta = -3$ is the case in which the average velocities of pumping and rotation are equal but opposite in direction), they tend to cancel each other and are quite large in magnitude before the instability thresholds are reached.

### 3.3. *General stability characteristics*

To study the general stability characteristics of Taylor–Dean flow, we consider wide ranges of $\mu$ and $\beta$, the two major parameters determining the basic flow. The prevalence of non-axisymmetric instability is evident by observing the results shown in figure 3 where instability modes varying from $m = 0$ to 8 can be identified. In this $(\mu, \beta)$-plane covering $-1 \leqslant \mu < 1$ and $-10 \leqslant \beta \leqslant 10$, the resolutions of both $\Delta\mu$ and $\Delta\beta$ are up to 0.1; therefore, in total 1420 cases of different $(\mu, \beta)$ are considered. Each case (or point) corresponding to a non-axisymmetric mode is represented by a particular marker (see the caption of the figure) and the point for the axisymmetric

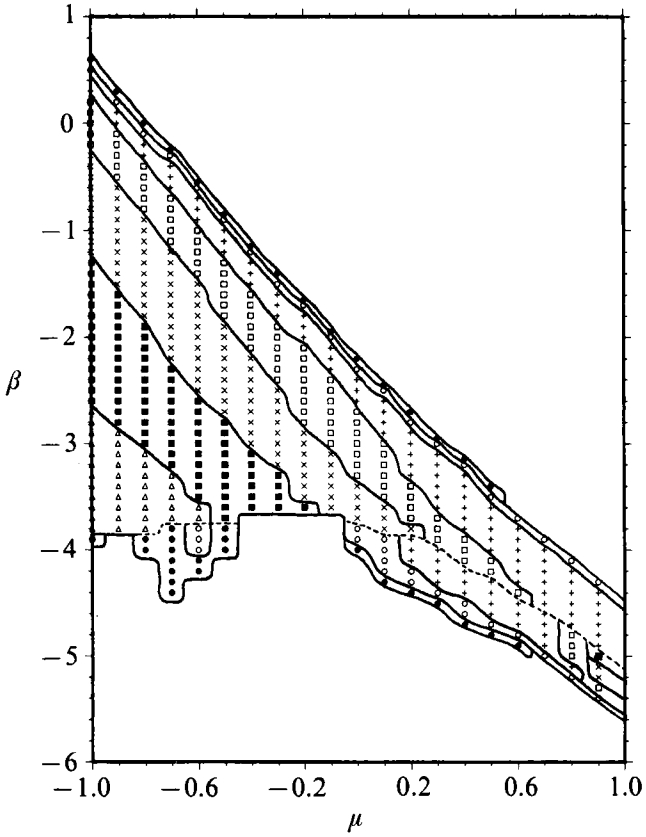


FIGURE 3. Map of non-axisymmetric modes in the $(\mu, \beta)$-plane: ——, boundary between different modes; – – –, boundary between the modes with opposite angular velocity; ●, $m = 1$; ○, $m = 2$; +, $m = 3$; □, $m = 4$; ×, $= 5$; ■, $m = 6$; △, $m = 7$; ⊕, $m = 8$.

mode is not marked. The solid curve accounts for the boundary between different modes and the dot curve represents the boundary dividing the modes with opposite-travelling wave direction.

A few typical cases in figure 3 concerning mode changing are worth noting. We first examine the case $\beta = 0$, the Taylor problem as considered by Krueger *et al.* (1966). It is found that the instability mode becomes non-axisymmetric with $m = 1$ at $\mu = -0.78$, and changes into other modes with higher $m$ as $\mu$ decreases. The values of $\mu$ corresponding to the mode changing agree excellently with those obtained by Krueger *et al.* (see also table 1 for comparison of other data). We now examine the cases of fixed $\mu$ and varying $\beta$. For $\mu = -1$, as $\beta$ decreases, the instability mode becomes non-axisymmetric with $m = 1$ at $\beta = 0.6$, and changes into $m = 2$ at 0.5, $m = 3$ at 0.4, $m = 4$ at 0.2, $m = 5$ at $-0.3$, $m = 6$ at $-1.3$, $m = 7$ at $-2.7$, $m = 8$ at $-3.9$, and becomes axisymmetric again at $-4.0$. The non-axisymmetric modes all travel in the same direction as the inner cylinder rotation. For $\mu = -0.5$, the instability mode becomes non-axisymmetric with $m = 1$ at approximately $\beta = -0.8$ (more precisely $-0.85$), and changes into different modes of $m = 2$, 3, 4, 5, and 6 as $\beta$ decreases to $-0.9$, $-1$, $-1.3$, $-1.9$, and $-2.8$, respectively. In $-3.8 < \beta < -3.7$, the mode switches between $m = 6$ and 1 with opposite-travelling wave direction. For larger $\mu$, the sequences of the mode-changing due to decreasing $\beta$ are, for instance, 1–2–3–4–5–2–1 for $\mu = 0$, 1–2–3–4–3–2–1 for $\mu = 0.5$, 2–3–3–2 for $\mu = 0.7$, and

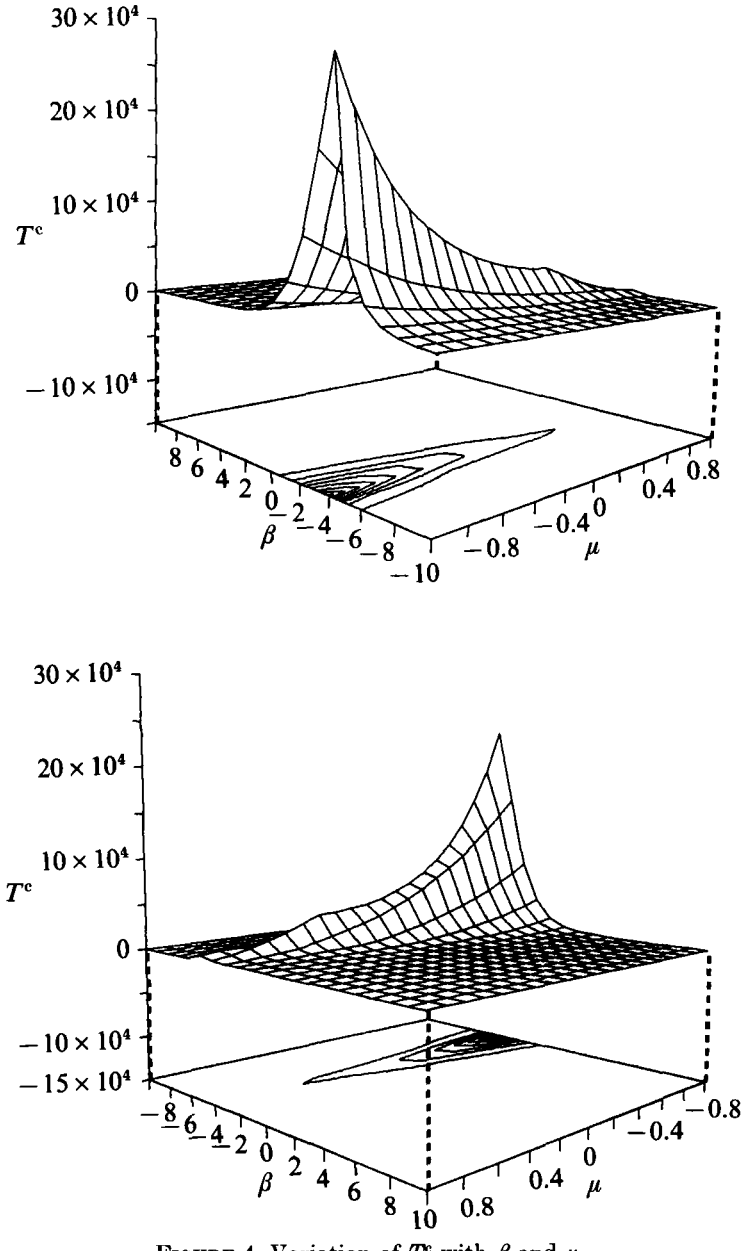


FIGURE 4. Variation of $T^c$ with $\beta$ and $\mu$.

2–3–6–5–4–2 for $\mu = 0.9$, and so on. From these sequences one can see that increasing $\mu$ reduces the number of mode changes except for $\mu$ close to 1. It is also noted that, as the travelling wave direction is the same as that of inner cylinder rotation (i.e. positive $c$ or negative $\sigma_r$), the azimuthal wavenumber $m$ generally increases as $\mu$ decreases, whereas the $m$–$\mu$ relation is reversed as the travelling wave and inner cylinder move in opposite directions.

The variation of $T^c$ and $a^c$ versus varying $\mu$ and $\beta$ are present by three dimensional plots in figures 4 and 5, respectively. The constant level contours with increments $\Delta T^c = 20000$ and $\Delta a^c = 1$ are also shown in the $(\mu, \beta)$-plane to make the data more

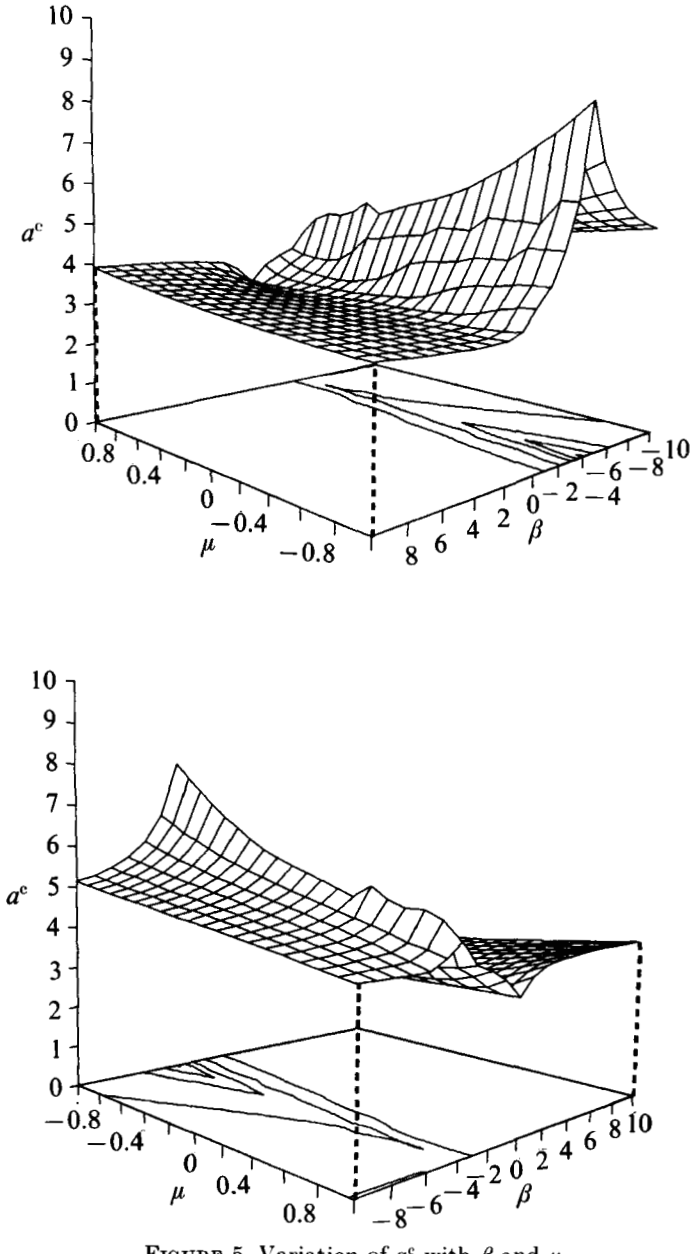


FIGURE 5. Variation of $a^c$ with $\beta$ and $\mu$.

traceable. As shown in figure 4, $T^c$ is generally a monotone decreasing function of $\mu$ for all the $\beta$ considered. On the other hand, for a fixed $\mu$, $T^c$ first increases with $\beta$, reaches a maximum, then decreases. Owing to the insufficient resolution of $\Delta\beta$ ($= 1$ in figures 4 and 5), the difference between the $\beta_{max}$ of various $\mu$ is not clearly demonstrated. As with the raw data along with figure 3, we found that the $\beta_{max}$ is either on the lower boundary dividing the axisymmetric and non-axisymmetric modes or on the dotted curves in figure 3. Namely, for $\mu < 0.3$, the $\beta_{max}$ is within $-3.9 < \beta < -3.6$; while for $\mu > 0.3$, the relation between $\mu$ and $\beta_{max}$ is approximately linear, governed by $-\beta_{max} \approx 1.59\mu + 3.5$.

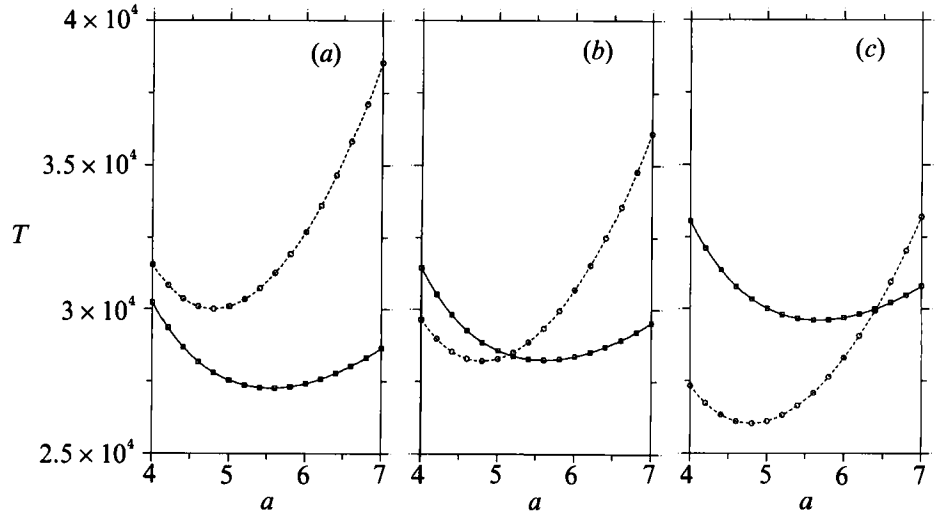


FIGURE 6. Neutral curves of different modes for $\mu = -1$ and various $\beta$: —□—, $m = 8$; ---○---, $m = 0$. (*a*) $\beta = -3.9$; (*b*) $\beta = -3.934$; (*c*) $\beta = -3.95$.

Figure 5 illustrates that $a^c$ increases monotonically with $\mu$ for approximately $\beta > 1$ and becomes decreasing otherwise except very near $\beta = 4.2$, where $a^c$ increases slightly with $\mu$ near $\mu = 0.3$. It also shows that, for all the $\mu$ considered, $a^c$ first increases with $\beta$, reaches a maximum, then decreases dramatically to a minimum, and eventually increases slightly for larger $\beta$. Generally, the maxima of both $T^c$ and $a^c$ occur at the same $(\mu, \beta)$. One also notes that for a fixed $\mu$, both $T^c$ and $a^c$ increase with $m$; namely, the instability mode with higher $m$ is of greater stability and smaller critical axial wavelength.

It is also worth reporting the nature of the neutral curves. There are two kinds of neutral curve for the present problem. One curve illustrates the variation of $T$ with $a$ and the other accounts for the relation between $T$ and $m$. The neutral curve in the $(T, a)$-plane for a non-axisymmetric instability mode is unimodal. However, as the change of instability mode occurs, the neutral curve consists of two branches, each of which accounts for a mode with different azimuthal wavenumber $m$ and, accordingly, the neutral curve is bimodal. The bimodal instability corresponds to a finite jump of $a^c$ (figure 6). The relation between $T$ and $m$ for $\mu = -1$ is shown in figure 7, for example, which presents the values of $T^c/T_0^c$ for various $m$ and several selected values of $\beta$ (where $T_0^c$ is the critical Taylor number of $m = 0$). The points connected by a continuous curve are associated with the same value of $\beta$. For $\beta = 1$, $T^c/T_0^c$ is a monotone increasing function of $m$, and $m = 0$ is the most unstable mode. The $m$ associated with the minimum of $T^c/T_0^c$ increases as $\beta$ decreases. For $\beta = -3.8$, the most unstable mode is $m = 8$. Note that for these cases in $\beta > \beta_{\max} = -3.934$, the $T^c$ of different modes vary greatly. But this is not the case for $\beta < \beta_{\max}$. For instance, as $\beta$ decreases to $-4$, the mode of $m = 0$ is most unstable but the values of $T^c/T_0^c$ of all modes with different $m$ are quite close. Similar results obtained for the cases of different $\mu$ considered. Generally, the cases for which the similarity of the $T^c$ of different modes holds are those located in the region below the curve of figure 3 associated with the maximum of $T^c$. In fact, in addition to $T^c$, the similarity between modes of different $m$ also holds for $a^c$, $c$ and its disturbance velocities in both the radial and azimuthal directions. This similarity of stability features is absent from either Taylor or Dean flow.

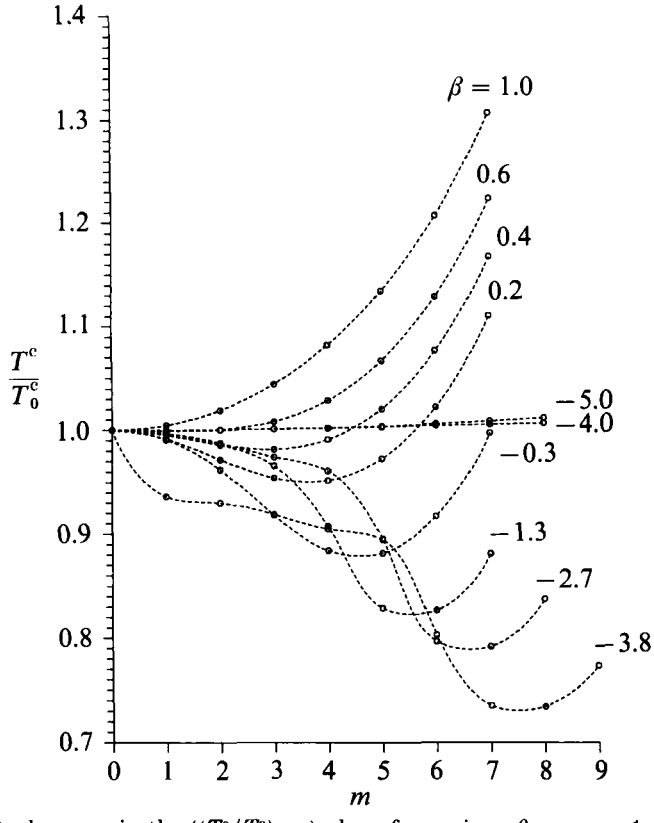


FIGURE 7. Neutral curves in the $((T^c/T_0^c), m)$-plane for various $\beta$ as $\mu = -1$; where $T_0^c$ is the $T^c$ value for $m = 0$.

## 4. Summary

We have conducted a complete analysis for the onset of secondary motion of Taylor–Dean flow in a small-gap spacing between two infinitely long rotating cylinders. We first show that previous investigations for the stability of small-gap Taylor–Dean flow were incomplete owing to the lack of consideration of the existence of non-axisymmetric oscillatory modes which in reality prevail in wide ranges of both $\mu$ and $\beta$. In particular, the peculiar neutral curves of $m = 0$ for near $\beta^* = -3.667$ presented by Hughes & Reid (1964) are replaced by the neutral curve of $m = 5$, which is unimodal and most unstable. We then identify the instability mode for each $(\mu, \beta)$ pair in the $(\mu, \beta)$-plane which covers $-1 \leqslant \mu < 1$ and $-10 \leqslant \beta \leqslant 10$. The range of $\beta$ in which the non-axisymmetric modes predominate decreases with increasing $\mu$. For a fixed $\mu$, the mode with higher $m$ is of greater stability and smaller axial wavelength; the most stable state with smallest axial wavelength occurs at a $\beta$ at which the travelling wave changes its direction. When the instability mode is changing into the other mode, the neutral curve in terms of $T$ and $a$ consists of two connected branches, each of which accounts for the neutral curve of different $m$. For $\beta < \beta_{max}$, modes with different azimuthal wavenumber $m$ are of similar stability characteristics in terms of $T^c$, $a^c$, $c$, and associated eigenfunctions of disturbance velocities.

The financial support for this work from National Science Council through Grant No. NSC 81-0401-E-002-503 is gratefully acknowledged.

## REFERENCES


BREWSTER, D. B., GROSBERG, P. & NISSAN, A. H. 1959 *Proc. R. Soc. Lond.* A**251**, 76.

BREWSTER, D. B. & NISSAN, A. H. 1958 *Chem. Eng. Sic.* **7**, 215.

CHANDRASEKHAR, S. 1961 *Hydrodynamic and Hydromagnetic Stability.* Clarendon.

CHEN, K. S., KU, A. C., CHAN, T. M. & YANG, S. Z. 1990 *J. Fluid Mech.* **213**, 149.

COUETTE, M. 1890 *Ann. Chim. Phys.* **21**, 433.

DEAN, W. R. 1928 *Proc. R. Soc. Lond.* A**121**, 402.

DIPRIMA, R. C. 1955 *Q. Appl. Maths* **13**, 55.

DIPRIMA, R. C. 1959 *J. Fluid Mech.* **6**, 462.

HAMMERLIN,. G. 1958 *Arch. Rat. Mech. Anal* **1**, 212.

HARRIS, D. L. & REID, W. H. 1964 *J. Fluid Mech.* **20**, 95.

HUGHES, T. H. & REID, W. H. 1964 *Z. Angew. Math. Phys.* **15**, 573.

KACHOYAN, B. J. 1987 *Z. Angew. Math. Phys.* **38**, 905.

KOMADA, A. Y. 1983 *Kawasaki Steel Tech. Rep.* vol. 8, p. 17.

KRUEGER, E. R., GROSS, A. & DIPRIMA, R. C. 1966 *J. Fluid Mech.* **24**, 521.

KURZWEG, U. H. 1963 *Z. Angew. Math. Phys.* **14**, 380.

MEISTER, B. 1962 *Z. Angew. Math. Phys.* **13**, 83.

MUTABAZI, I., HEGSETH, J. J., ANDERECK, C. D. & WESFREID, J. E. 1988 *Phys. Rev.* A**38**, 4752.

MUTABAZI, I., HEGSETH, J. J., ANDERECK, C. D. & WESFREID, J. E. 1990 *Phys. Rev. Let.* **64**, 1729.

MUTABAZI, I., NORMAND, C., PEERHOSSAINI, H. & WESFREID, J. E. 1989 *Phys. Rev.* A**39**, 763.

MUTABAZI, I., WESFREID, J. E., HEGSETH, J. J. & ANDERECK, C. D. 1991 *Eur. J. Mech.* B/*Fluids* **10**, 239.

NABATAME, M. 1984 *Nippon Kokan Tech. Rep.* (*Overseas*) vol. 40, p. 9.

POWELL, M. J. D. 1970 *Numerical Methods for Nonlinear Algebraic Equations* (ed. P. H. Rabinowitz). Gordon and Breach.

RANEY, D. C. & CHANG, T. S. 1971 *Z. Angew. Math. Phys.* **22**, 680.

RAYLEIGH, LORD 1916 *Proc. R. Soc. Lond.* A**93**, 148.

REID, W. H. 1958 *Proc. R. Soc. Lond.* A**244**, 186.

SPARROW, E. M. & LIN, S. H. 1965 *Phys. Fluids* **8**, 229.

SPARROW, E. M, MUNRO, W. D. & JONSSON, V. K. 1964 *J. Fluid Mech.* **20**, 35.

TAYLOR, G. I. 1923 *Phil. Trans. R. Soc. Lond.* A**223**, 289.

VOHR, J. H. 1968 *Trans. ASME* F: *J. Lubrication Tech.* **11**, 285.

WALOWIT, J., TSAO, S. & DIPRIMA, R. C. 1964 *Trans. ASME* E: *J. Appl. Mech.* **86**, 585.